

LETTER

Coupled predator–prey oscillations in a chaotic food web

Elisa Benincà,^{1,2} Klaus D. Jöhnk,^{1,3} Reinhard Heerkloss⁴ and Jef Huisman^{1*}

¹Aquatic Microbiology, Institute for Biodiversity and Ecosystem Dynamics, University of Amsterdam, Nieuwe

Achtergracht 127, 1018 WS Amsterdam, The Netherlands

²Department of Aquatic Ecology and Water Quality

Management, University of Wageningen, Wageningen, The Netherlands

³Leibniz-Institute of Freshwater Ecology and Inland Fisheries, Neuglobsow, Germany

⁴Institute of Biosciences, University of Rostock, Albert Einstein Str 3, D-18051 Rostock, Germany

*Correspondence: E-mail: j.huisman@uva.nl

Abstract

Coupling of several predator–prey oscillations can generate intriguing patterns of synchronization and chaos. Theory predicts that prey species will fluctuate in phase if predator–prey cycles are coupled through generalist predators, whereas they will fluctuate in anti-phase if predator–prey cycles are coupled through competition between prey species. Here, we investigate predator–prey oscillations in a long-term experiment with a marine plankton community. Wavelet analysis of the species fluctuations reveals two predator–prey cycles that fluctuate largely in anti-phase. The phase angles point at strong competition between the phytoplankton species, but relatively little prey overlap among the zooplankton species. This food web architecture is consistent with the size structure of the plankton community, and generates highly dynamic food webs. Continued alternations in species dominance enable coexistence of the prey species through a non-equilibrium ‘killing-the-winner’ mechanism, as the system shifts back and forth between the two predator–prey cycles in a chaotic fashion.

Keywords

Biodiversity, chaos, coupled oscillators, food web, plankton community, predator–prey cycles, time series analysis, wavelet analysis.

Ecology Letters (2009) 12: 1367–1378

INTRODUCTION

In 1665, confined to his home by a minor illness, the Dutch physicist Christiaan Huygens discovered an ‘odd kind of sympathy’ between two pendulum clocks mounted next to each other on the same beam (Bennett *et al.* 2002). The two pendula oscillated with exactly the same frequency, but in opposite directions. When he disturbed one pendulum, the anti-phase oscillations were quickly restored. Apparently, the two pendula displayed coupled oscillations. Since Huygens’s discovery, coupled oscillations have been described in many biological, chemical and physical systems (Strogatz & Stewart 1993; Golubitsky *et al.* 1999; Rodriguez *et al.* 1999; Kiss *et al.* 2002). In food webs, resource–consumer interactions can generate oscillations, for instance in the form of predator–prey and host–parasitoid cycles. In a series of papers, Vandermeer (1993, 2004, 2006) showed that coupling of several predator–prey oscillations can lead to intriguing patterns of synchronization, as in Huygens’s clockwork.

Vandermeer (2004) described two different ways in which several predator–prey oscillations can be coupled. If specialist predators each feed on only one prey species while these prey species compete with each other, we say that the predator–prey systems are ‘coupled through competition’ (Fig. 1a). Conversely, if generalist predators feed on all prey species, we say that the predator–prey systems are ‘coupled through predation’ (Fig. 1b). Interestingly, theory predicts that the mode of coupling affects the phase relationships between the species fluctuations. Prey species are predicted to oscillate all in phase with each other if predator–prey systems are coupled through generalist predation only. In contrast, prey species are predicted to oscillate in anti-phase if systems are coupled through competition only. Anti-phase oscillations are characterized by continued alternations in species dominance, such that the dominance of one prey species is followed by the dominance of another prey species, and so on. Likewise, predators are predicted to oscillate in phase if systems are coupled through predation, but in anti-phase

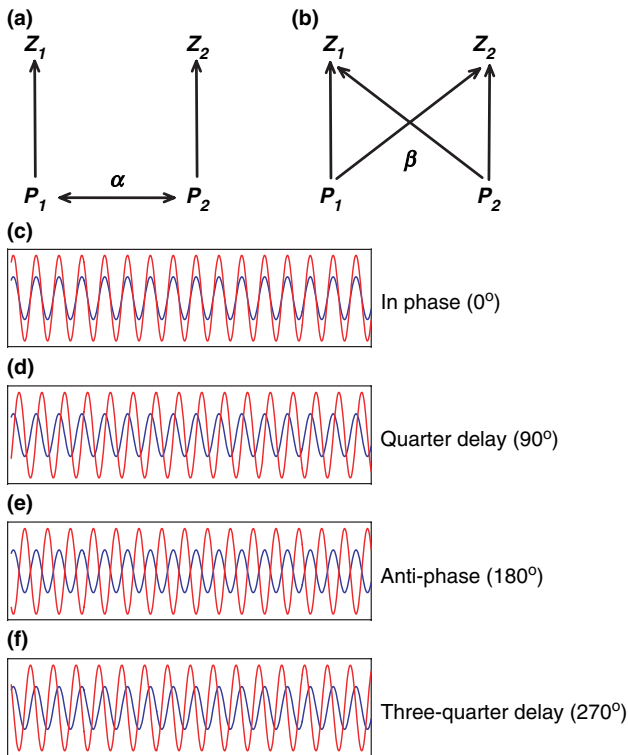


Figure 1 Coupling of two predator–prey systems. (a) Coupling through competition: two specialist predators each feed on only one prey species, while the prey species (P_1 and P_2) interact through competition. The magnitude of the competition coefficient α is a measure of the strength of coupling. (b) Coupling through predation: two generalist predators (Z_1 and Z_2) feed on both prey species. The magnitude of the selectivity coefficient β is a measure of the strength of coupling (note that high β implies low selectivity). (c–f) Coupled oscillations may lead to different phase angles between the species fluctuations: (c) in-phase oscillations (0°); (d) quarter delay oscillations (90°); (e) anti-phase oscillations (180°); (f) three-quarter delay oscillations (270°).

if systems are coupled through competition (Vandermeer 2004).

In reality, of course, predator–prey systems will often be coupled through both competition and predation. In this mixed case, theory predicts that the population dynamics become chaotic for a relatively wide range of parameter values (Vandermeer 2004). Hence, species fluctuations will not display the strict regularity of Huygens's clockwork but will vary in frequency and amplitude, which makes it more difficult to identify patterns of synchrony. Still, some predator–prey systems may be coupled predominantly through competition, whereas others may be coupled mainly through predation, and the signatures of these different coupling modes may still be reflected in the phase relationships between the species (Vandermeer 2004).

With these intriguing model predictions in mind, the question is whether similar patterns of in-phase and anti-phase synchrony can be observed in real food webs. Recently, we demonstrated chaos in a long-term experiment with a plankton community (Benincà *et al.* 2008). The plankton community was isolated from the Baltic Sea, and consisted of phytoplankton species, herbivorous and predatory zooplankton species, and a microbial loop. It was maintained in a laboratory mesocosm for more than 8 years. Despite constant laboratory conditions, the species abundances fluctuated over several orders of magnitude. We showed that the predictability of these species fluctuations was limited to a time horizon of only 15–30 days (Benincà *et al.* 2008). However, we were unable to pinpoint the underlying mechanisms causing these chaotic fluctuations. Mathematical models suggest several possible mechanisms that can generate chaos in plankton communities, including multispecies competition (Huisman & Weissing 1999, 2001), tritrophic interactions (Hastings & Powell 1991), coupled predator–prey oscillations (Vandermeer 2004; Dakos *et al.* 2009), intraguild predation (Tanabe & Namba 2005), and the interplay between mixing and sinking of plankton populations (Huisman *et al.* 2006).

In this study, we compare the results of this long-term experiment with predictions of the coupled predator–prey model of Vandermeer (2004). For this purpose, we use a simple statistical test to establish whether the experimental time series is characterized by alternations in species dominance. In addition, we apply an advanced statistical technique, known as cross-wavelet analysis (Torrence & Compo 1998; Grinsted *et al.* 2004), to investigate the phase relationships between the dominant phytoplankton and zooplankton species. The analyses show that the chaotic ups and downs of the species are essentially driven by two coupled predator–prey cycles fluctuating largely in anti-phase. This presents the first experimental demonstration of two coupled oscillations in a chaotic food web.

THEORY

Consider a simple food web model consisting of two coupled predator–prey systems. Let P_1 and P_2 denote the two prey species, and Z_1 and Z_2 the two predator species. We assume that the prey species interact through Lotka–Volterra competition, and are consumed by the predators according to a saturating functional response. The model can then be written as (Rosenzweig & MacArthur 1963; Vandermeer 2004; Dakos *et al.* 2009):

$$\frac{dP_i}{dt} = r_i P_i \left(1 - \frac{\sum_j \alpha_{ij} P_j}{K_i} \right) - \sum_k \frac{g_k \beta_{ik} P_i}{H_k + \sum_j \beta_{jk} P_j} Z_k \quad i = 1, 2 \quad (1)$$

$$\frac{dZ_k}{dt} = \frac{g_k \sum_j \beta_{jk} P_j}{H_k + \sum_j \beta_{jk} P_j} Z_k - m_k Z_k \quad k = 1, 2 \quad (2)$$

Here, r_i is the specific growth rate of prey species i and K_i is its carrying capacity, the competition coefficients α_{ij} describe competition between the two prey species, g_k is the maximum specific grazing rate of predator species k and H_k is its half-saturation constant, β_{ik} is the selectivity coefficient of predator species k for prey species i (where $0 \leq \beta_{ik} \leq 1$), and m_k is the specific mortality rate of the predator species. Without loss of generality, we scale the model equations such that intraspecific competition equals unity ($\alpha_{11} = \alpha_{22} = 1$) and that predators have maximum selectivity for their preferred prey species ($\beta_{11} = \beta_{22} = 1$). For the purpose of illustration, we simplify the model by assuming symmetric competition between the prey species ($\alpha_{12} = \alpha_{21} = \alpha$) and symmetric selectivity of predators for their less-preferred prey species ($\beta_{12} = \beta_{21} = \beta$).

The coupling between the two predator–prey systems is now captured by two coefficients, α and β (Vandermeer 2004). If $\alpha = \beta = 0$, the prey species do not compete and the predator species consume only their preferred prey species. The two predator–prey systems are thus independent of each other. If $\alpha > 0$, the prey species compete and we say that the two predator–prey systems are coupled through competition (Fig. 1a). Conversely, if $\beta > 0$, both predators feed on both prey species. In this case, we say that the predator–prey systems are coupled through predation (Fig. 1b).

MATERIAL AND METHODS

Long-term experiment

We investigated coupled oscillations between predators and prey species in a long-term experiment with a plankton community isolated from the Baltic Sea (Heerkloss & Klinkenberg 1998; Benincà *et al.* 2008). Figure 2 shows the food web structure of this plankton community. Phytoplankton was divided in three functional groups: picophytoplankton consisting of 1–2 μm picocyanobacteria (mostly *Synechococcus* species), nanophytoplankton consisting of 3–5 μm eukaryotic flagellates (mainly *Rhodomonas lacustris* Pascher and Ruttner), and large filamentous diatoms (*Melosira moniliformis* (O.F.M.) C. Agardh). Herbivorous zooplankton was also classified into three groups: protozoa (mainly large ciliates such as *Cyclidium* and *Strombidium* species), rotifers (mainly *Brachionus plicatilis* (O.F.M.)), and the calanoid copepod *Eurytemora affinis* (Poppe). Feeding relationships of the species are indicated by arrows in Fig. 2. Previously, we assumed that rotifers fed mainly on nanoflagellates, and to a lesser extent on picocyanobacteria, based on the correlations between their species abundances

(Benincà *et al.* 2008). However, the phase relationships reported in this paper (see Results) suggest that rotifers fed mainly on picocyanobacteria, and to a lesser extent on nanoflagellates. Rotifers and protozoa were eaten by cyclopoid copepods. The microbial loop was represented by heterotrophic bacteria and two groups of detritivores (ostracods and harpacticoid copepods).

The experiment started on 31 March 1989, when the mesocosm was filled with a 10 cm sediment layer and 90 L of water from the Darss-Zingst estuary (southern Baltic Sea; 54°26' N, 12°42' E). This inoculum provided the plankton community for the entire experiment, which was maintained at a temperature of $\sim 20^\circ\text{C}$, salinity of $\sim 9\text{‰}$, incident irradiation of $50 \mu\text{mol photons m}^{-2} \text{s}^{-1}$ with a 16 h: 8 h light-dark cycle, and constant aeration for more than 8 years (Heerkloss & Klinkenberg 1998; Benincà *et al.* 2008). The population abundances of the species were counted twice a week, from 12 July 1990 until the experiment was terminated on 20 October 1997. From 23 November 1990 to 5 March 1991, however, the length of the light period was temporarily reduced from 16 to 12 h per day (Heerkloss & Klinkenberg 1998). Wavelet analysis does not require stationary time series. Therefore, we decided to make use of the entire time series, including these few months with a reduced light period. This resulted in a time series of 2657 days, which is 338 days longer than the time series analysed previously (Benincà *et al.* 2008). Further details of the mesocosm experiment are provided in the Supplementary Information of Benincà *et al.* (2008).

In this study, we are particularly interested in the phytoplankton and herbivorous zooplankton, because their ups and downs resembled typical predator–prey oscillations (Benincà *et al.* 2008). Of these species, picocyanobacteria, nanoflagellates, rotifers and calanoid copepods were present in large numbers during the entire experiment, whereas the time series of filamentous diatoms and protozoa contained long sequences of zero values. This does not imply that filamentous diatoms and protozoa were completely absent from the food web, but at least their concentrations remained below the detection limit during most of the experimental period. We therefore focus specifically on picocyanobacteria, nanoflagellates, rotifers and calanoid copepods (Fig. 2). We applied nearly the same data transformation as in Benincà *et al.* (2008). First, we interpolated each time series using cubic hermite interpolation, to obtain data with equidistant time intervals of 3.35 days. As a result, the time series contains 794 data points for each species. Next, the time series were rescaled by a fourth-root power transformation to suppress sharp peaks that may obscure less conspicuous periodicities. Contrary to Benincà *et al.* (2008), however, we did not detrend the time series, because wavelet analysis can handle non-stationary data. The complete data set, containing both

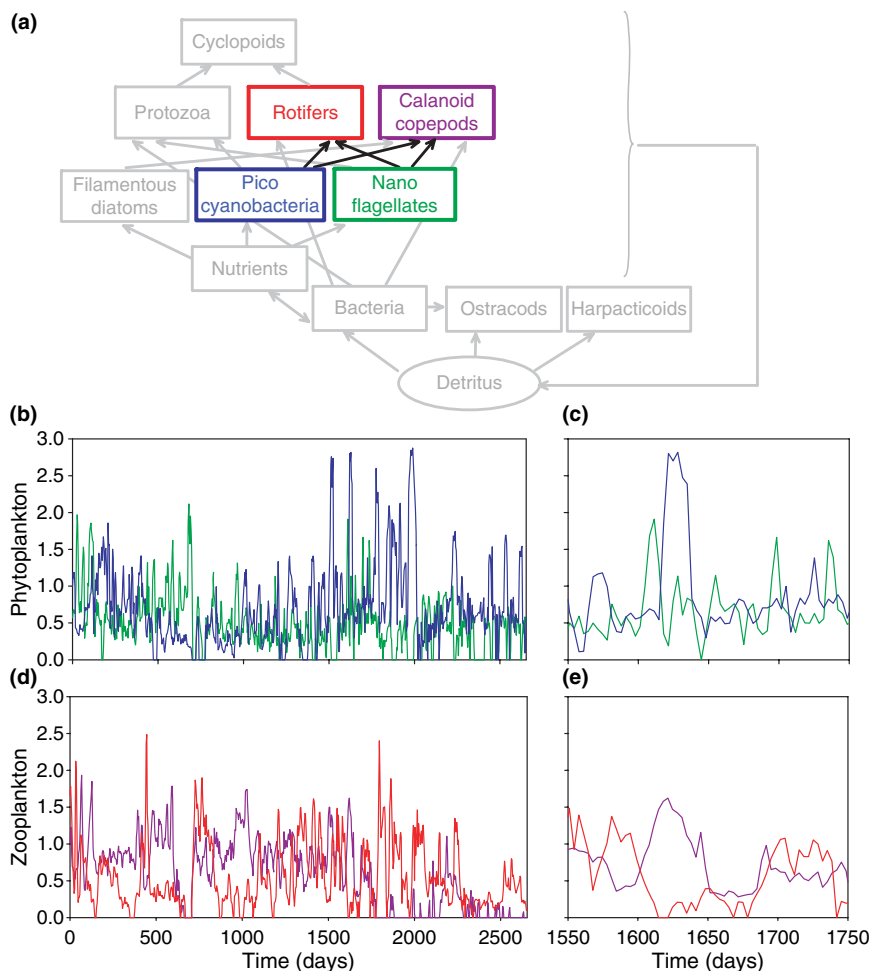


Figure 2 Experimental data. (a) Food web structure of the mesocosm experiment. Our analysis focuses on coupled oscillations between picocyanobacteria (mainly *Synechococcus* spp.), nanoflagellates (mainly *Rhodomonas lacustris*), rotifers (mainly *Brachionus plicatilis*), and calanoid copepods (*Eurytemora affinis*). (b) Time series of picocyanobacteria (blue) and nanoflagellates (green). (c) Close-up of the species fluctuations shown in panel b. (d) Time series of rotifers (red) and calanoid copepods (purple). (e) Close-up of the species fluctuations shown in panel d. The time series were transformed by a fourth-root power transformation to suppress sharp peaks, and hence phytoplankton and zooplankton abundances are expressed as $(\text{mg fw L}^{-1})^{1/4}$.

the original and the transformed time series, is made available in Appendix S1 of the Supporting Information.

Alternations in species dominance

We tested for alternations in species dominance simply by counting the number of times that a peak of one phytoplankton species was followed by a peak of the other phytoplankton species. Therefore, we searched all local maxima in the transformed time series of a species, and identified these local maxima as 'peaks' if they were at least 0.2 units higher than nearby local minima and at least 12 days spread apart. Our null hypothesis is that the species identity of peaks is randomly distributed. Hence, since both phytoplankton species had approximately the same number of peaks in the time series, the probability that two consecutive phytoplankton peaks are dominated by the same species would be 0.5. This can be tested against the alternative hypothesis that two consecutive peaks are more likely to be dominated by different species using the binomial distribution $B(n, 0.5)$, where n is the total number

of phytoplankton peaks in the time series. The same test was applied to the two zooplankton species.

Wavelet analysis

We investigated the species fluctuations in further detail using wavelet analysis, a powerful statistical technique for the analysis of periodic signals in non-stationary time series (Torrence & Compo 1998; Cazelles *et al.* 2008). Traditionally, periodic signals in time series are analysed by spectral analysis. However, classic spectral analysis requires stationary time series. This limits the applicability of spectral analysis, because many ecological time series are not stationary but display temporal changes in their trends and fluctuations. This limitation is overcome by wavelet analysis, which is specifically tailored for the analysis of non-stationary time series. Wavelet analysis decomposes local fluctuations observed during a small stretch of time into a series of different frequencies (periods). This decomposition is based on a local wave function, known as the wavelet function, which captures the local fluctuations in terms of

both their time and frequency (period). Thus, wavelet analysis allows investigation of changes in the frequency distribution of species fluctuations during time. Given its applicability to non-stationary data, wavelet analysis is rapidly becoming a popular tool for the analysis of ecological time series (Grenfell *et al.* 2001; Keitt & Fisher 2006; Ménard *et al.* 2007; Keitt 2008). Appendix S2 in the Supporting Information presents a simple example illustrating the basic idea of wavelet analysis.

Cross-wavelet analysis is an extension of wavelet analysis. It compares the wavelet power spectra of two time series (Grinsted *et al.* 2004). This enables detection of similarities in the local fluctuations of the two time series, and allows estimation of the phase angles between these fluctuations. This makes cross-wavelet analysis a very useful technique for the study of predator–prey oscillations. To identify significant results, we investigated whether the cross-wavelet spectra of two time series were significantly different (at the 0.05 level) from the cross-wavelet spectra of two independent red-noise processes with the same first-order autoregression coefficients as the time series (Appendix S2; see also Grinsted *et al.* 2004). We used comparison against red noise, because the time series in our study showed a high degree of temporal autocorrelation (Gilman *et al.* 1963; Grinsted *et al.* 2004).

To investigate the robustness of our findings, we also applied a related method called wavelet coherence (Grinsted *et al.* 2004; Maraun & Kurths 2004). Wavelet coherence measures the coherence of the fluctuations in two time series by normalizing their cross-wavelet spectra by the product of the two single wavelet spectra. Thus, cross-wavelet analysis and wavelet coherence provide different perspectives on coupled fluctuations of two time series. While cross-wavelet analysis emphasizes the common power spectrum of two time series (i.e., the magnitude of the fluctuations), wavelet coherence emphasizes the correlations between the fluctuations of two time series (i.e., the coherence of the fluctuations). For more details on cross-wavelet analysis and wavelet coherence the interested reader is referred to Appendix S2.

RESULTS

Theoretical predictions

The model predicts that, if two predator–prey systems are coupled through predation only, the two prey species will fluctuate in phase (Fig. 3a). In this specific case, with $\alpha = 0$ and $\beta = 0.0015$, the two prey species fluctuated at a periodicity of ~ 40 days. Cross-wavelet analysis successfully captured these patterns (Fig. 3b). Colour coding in the contour plots indicates the local power of the cross-wavelet spectra. Black contour lines enclose regions of $>95\%$

confidence that the observed local cross-wavelet power exceeds the cross-wavelet power that would have been generated by two independent red-noise processes. Shaded areas on both sides of the contour plots represent the cone of influence, where edge effects might distort the signal. Therefore, we restrict our interpretation of the cross-wavelet spectrum to the non-shaded areas. According to the cross-wavelet spectrum, the two prey species fluctuated with high common power at a significant periodicity of 32–64 days (red band in Fig. 3b). In addition, cross-wavelet analysis also points at a slightly less significant periodicity of 16–32 days (yellow band in Fig. 3b), which is half the period of the actual fluctuations. Such harmonics are commonly observed in spectral analysis and wavelet analysis, if the waveform of the fluctuations is not perfectly sinusoidal. The arrows in the significant common power area all point to the right, which accurately reflect a phase angle of 0° between the fluctuations of the two prey species (Fig. 3b). We also applied cross-wavelet analysis to all other species combinations in this food web model. The results are summarized in Table 1. This shows that, analogous to the prey species, the two predator species also fluctuated in phase (i.e., at a phase angle of 0°), and that the prey species were tracked by fluctuations of the predators with a quarter delay (phase angle of 90°). A quarter delay between the fluctuations of predator and prey species is typical for many predator–prey models (e.g., Begon *et al.* 2006).

Coupling through competition only ($\alpha = 0.075$, $\beta = 0$) revealed a different pattern. In this case, the model predicts that the two prey species fluctuate almost in anti-phase (Fig. 3c). Cross-wavelet analysis reveals that the two prey species fluctuate again at a significant periodicity of 32–64 days, but the arrows now indicate a phase angle of $\sim 135^\circ$ (Fig. 3d, Table 1). Thus, interestingly, the oscillations produced by coupling through competition are not in perfect anti-phase (180°), but cover $3/8$ th (i.e., 135°) of the full circle. The phase angle distribution of the two prey species also points at a less significant periodicity of 16–32 days with a phase angle centred around 290° (Fig. 3d, Table 1), which is again explained by the non-sinusoidal waveform of the signal.

Models that include coupling through both competition and predation often display chaotic dynamics (Vandermeer 2004). In this case, the dynamics are still dominated by fluctuations with a periodicity of 32–64 days, but with clear variations in the phase relationships between the species (Fig. 3e). This is confirmed by cross-wavelet analysis, which detects the dominant periodicity of the species fluctuations, and shows that the phase angles vary in all directions (Fig. 3f). Still, some pattern in the distribution of the phase angles can be discerned. In this model example, coupling through competition was stronger than coupling through predation ($\alpha = 1.5$, $\beta = 0.1$), and therefore the chaotic

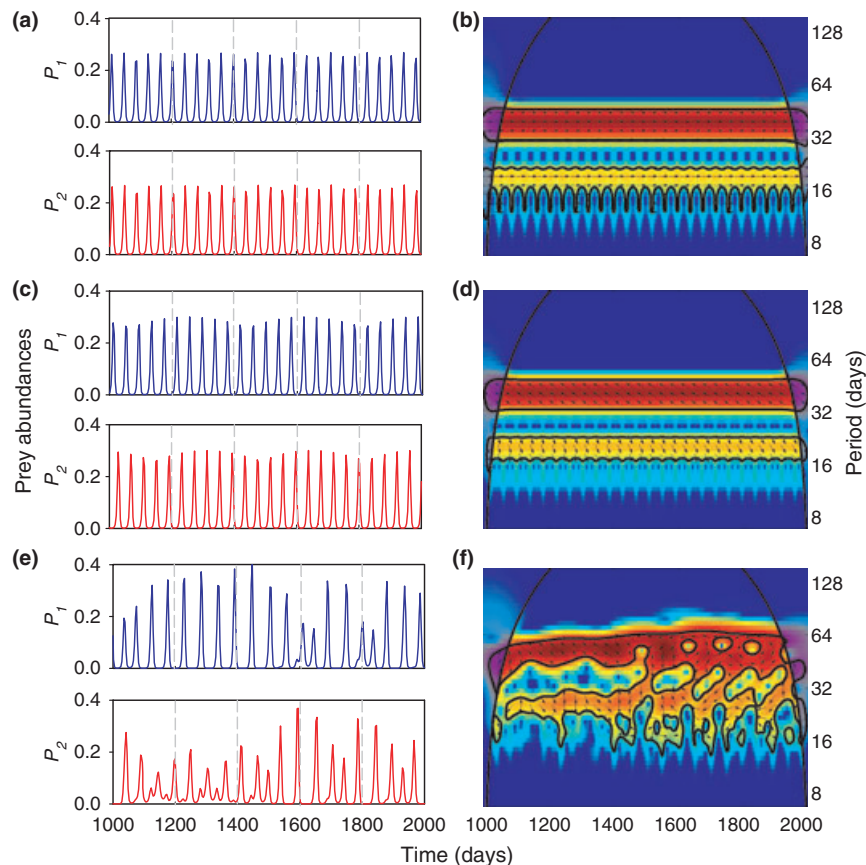


Figure 3 Model predictions. Time plots (left panels) and cross-wavelet spectra (right panels) of the two prey species, predicted by the model for various modes of coupling. (a–b) In case of coupling through predation only ($\alpha = 0$, $\beta = 0.0015$), the two prey species oscillate in phase (phase angle of 0°). (c–d) In case of coupling through competition only ($\alpha = 0.075$, $\beta = 0$), the two prey species oscillate almost in anti-phase (phase angle of 135°). (e–f) Coupling through both competition and predation ($\alpha = 1.5$, $\beta = 0.1$) may lead to chaotic population dynamics with a range of different phase angles between the two prey species. The cross-wavelet power spectra are presented as contour plots, where the y-axis plots the common periodicities in the fluctuations of the two prey species, and the x-axis plots how these common periodicities change over time. Colour coding indicates the cross-wavelet power (ranging from low power in blue to high power in red), which is a measure of the relatedness between the fluctuations of the two prey species. Black contour lines enclose significant regions in the cross-wavelet power spectra (i.e., regions of $>95\%$ confidence that the cross-wavelet power of the two prey species exceeds red noise). Arrows indicate the phase angles between the fluctuations of the two prey species, where arrows pointing to the right represent in-phase oscillations (0°) while arrows pointing to the left represent anti-phase oscillations (180°). Shaded areas on both sides of the contour plots represent the cone of influence, where edge effects might distort the signal. For more details on cross-wavelet analysis, see Appendix S2. Parameter values used in the simulations: $r_1 = r_2 = 1$, $K_1 = K_2 = 1$, $m_1 = m_2 = 0.1$, $g_1 = g_2 = 1.5$, $H_1 = H_2 = 0.8$. Initial conditions: $P_1 = 0.28$, $P_2 = 0.50$, $Z_1 = 0.14$, $Z_2 = 0.18$.

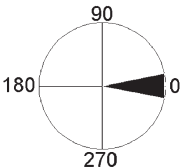
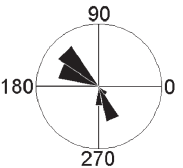
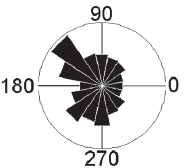
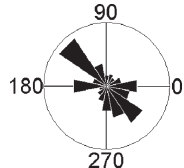
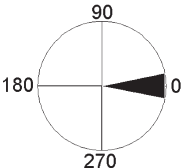
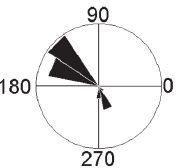
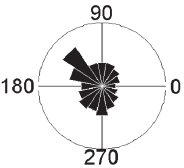
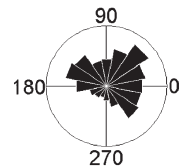
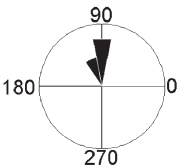
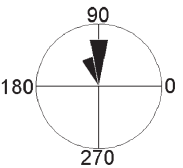
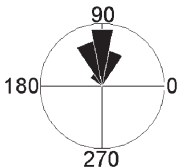
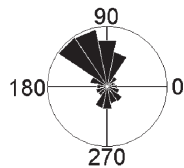
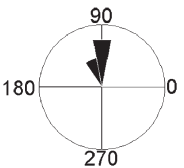
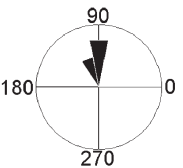
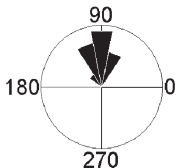
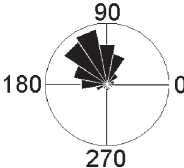
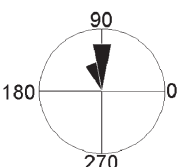
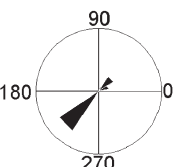
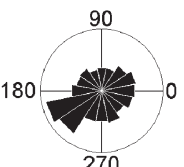
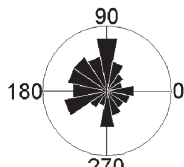
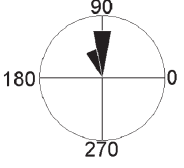
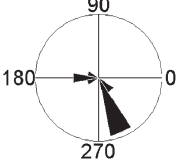
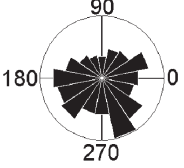
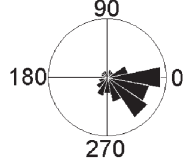
fluctuations of the two prey species were quite often in anti-phase with a main phase angle at $\sim 135^\circ$ (Fig. 3f; Table 1).

Experimental analysis

The mesocosm experiment showed strong fluctuations of the phytoplankton and zooplankton species (Fig. 2). A close look at the phytoplankton fluctuations suggests alternating dominance of picocyanobacteria and nanoflagellates (Fig. 2b,c). To quantify this observation, we identified the

species composition of all local phytoplankton peaks in the time series. This yielded 118 cases in which the phytoplankton species composition of consecutive peaks alternated between picocyanobacteria and nanoflagellates, and only 34 cases in which the phytoplankton species composition of consecutive peaks remained the same. These alternations in species composition deviate significantly from the null hypothesis that the peaks of picocyanobacteria and nanoflagellates are randomly distributed (i.e., the probability of drawing 118 or more cases from the binomial

Table 1 Relative frequency distributions of the phase angles between the fluctuating species

Species	Model predictions			Experiment
	<i>Coupling through predation</i>	<i>Coupling through competition</i>	<i>Mixture of both coupling modes</i>	<i>Mesocosm data</i>
Nanoflagellates (P_1) vs Picocyanobacteria (P_2)				
Calanoids (Z_1) vs Rotifers (Z_2)				
Nanoflagellates (P_1) vs Calanoids (Z_1)				
Picocyanobacteria (P_2) vs Rotifers (Z_2)				
Nanoflagellates (P_1) vs Rotifers (Z_2)				
Picocyanobacteria (P_2) vs Calanoids (Z_1)				

The relative frequency distributions are obtained from cross-wavelet spectra of the model predictions (Fig. 3) and experimental data (Fig. 4). We selected all phase angles located within significant regions of the cross-wavelet spectra but outside the cone of influence. The second, third, and fourth column show the phase angles predicted by the model, assuming coupling through predation ($\alpha = 0$; $\beta = 0.0015$), coupling through competition ($\alpha = 0.075$; $\beta = 0$), and the combination of both modes of coupling that gave the best fit between model predictions and experimental data ($\alpha = 1.5$; $\beta = 0.1$), respectively. The fifth column shows the phase angles detected in the experimental data.

distribution $B(152; 0.5)$ is $P < 0.001$). We found similar patterns in the zooplankton community (Fig. 2d,e), with 69 cases in which the zooplankton species composition of consecutive peaks alternated between rotifers and calanoid copepods, but only 33 cases in which the zooplankton species composition of consecutive peaks remained the same. Again, this pattern of alternating species composition deviates significantly from the null hypothesis that the peaks of rotifers and calanoid copepods are randomly distributed (the probability of drawing 69 or more cases from $B(102; 0.5)$ is $P < 0.001$).

As a next step, we investigated the species fluctuations using cross-wavelet analysis. The cross-wavelet spectrum shows that nanoflagellates and picocyanobacteria displayed coupled fluctuations with a significant periodicity of 32–64 days during the time periods from 1300 to 1700 days and from 1900 to 2100 days (Fig. 4a). Arrows in significant regions of the cross-wavelet spectrum point at anti-phase fluctuations of nanoflagellates and picocyanobacteria,

characterized by a main phase angle at $\sim 135^\circ$ and an additional phase angle at $\sim 315^\circ$. Both phase angles were also predicted by the model if the predator–prey systems would be coupled through competition (Table 1). Calanoid copepods and rotifers displayed coupled oscillations with a significant periodicity of 16–64 days from day 500 to 1700 (Fig. 4b). Significant regions in their cross-wavelet spectrum reveal a wide distribution of different phase angles, with dominant phase angles at $\sim 45^\circ$ and at $135\text{--}157^\circ$. The latter angle is close to the phase angle predicted for predator–prey systems coupled through competition (Table 1).

Phase angles of picocyanobacteria vs. rotifers and of nanoflagellates vs. calanoid copepods pointed at $90\text{--}135^\circ$ (Fig. 4c,d; Table 1). Thus, we observed roughly a quarter delay between fluctuations of predators and their preferred prey species, consistent with the phase angle of 90° predicted by the model irrespective of the mode of coupling. Rotifers and their less-preferred prey (nanoflagellates) also showed coupled oscillations; their phase angles

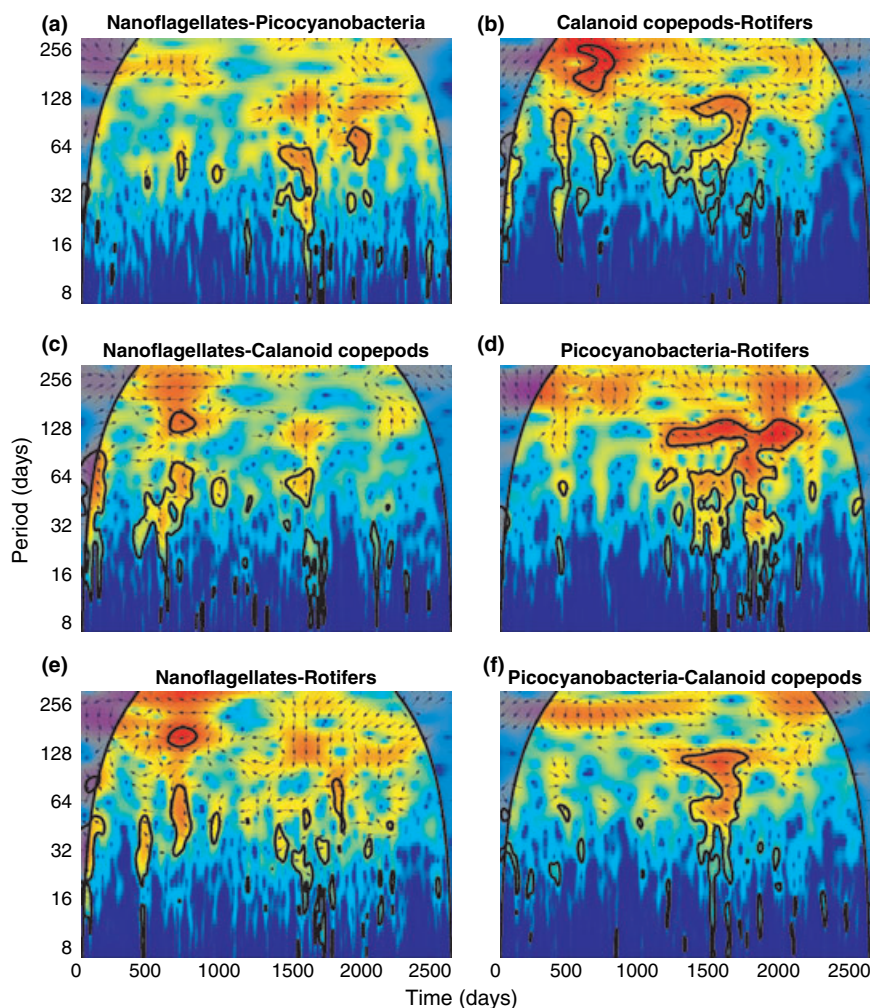


Figure 4 Cross-wavelet spectra of the experimental data. (a) Nanoflagellates vs. picocyanobacteria (P_1 vs. P_2); (b) calanoid copepods vs. rotifers (Z_1 vs. Z_2); (c) nanoflagellates vs. calanoid copepods (P_1 vs. Z_1); (d) picocyanobacteria vs. rotifers (P_2 vs. Z_2); (e) nanoflagellates vs. rotifers (P_1 vs. Z_2); (f) picocyanobacteria vs. calanoid copepods (P_2 vs. Z_1). Colour coding indicates the cross-wavelet power, while arrows indicate the phase angles between the fluctuations of the two time series (as in Fig. 3). Black contour lines enclose significant regions in the cross-wavelet power spectra. Shaded areas on both sides of the contour plots represent the cone of influence, where edge effects might distort the signal (see Appendix S2).

point to a range of different directions, but phase angles at $\sim 90^\circ$ and $\sim 202^\circ$ seem dominant (Fig. 4e; Table 1). Interestingly, the phase angle of $\sim 90^\circ$ is consistent with coupling through predation, while the phase angle of 202° is consistent with coupling through competition. The phase angles of calanoid copepods and their less-preferred prey (picocyanobacteria) are far from the phase angle of 90° predicted by coupling through predation, but close to the phase angle of 293° predicted by coupling through competition (Fig. 4f; Table 1).

Time series analysis by wavelet coherence demonstrated significant coherence in the species fluctuations during at least part of the time series (Fig. S4 in Appendix S2), meaning that the ups and downs of the different species in the plankton community were indeed related with each other. Moreover, wavelet coherence detected similar phase angles between the species fluctuations as cross-wavelet analysis (Table S1). This confirms the consistency of our results.

Comparison between theoretical predictions and experimental data

To investigate these patterns in further detail, we ran many model simulations using different strengths of coupling (i.e., different combinations of α and β). More specifically, we screened the entire parameter space that allowed coexistence of all four species in the model ($0 \leq \alpha \leq 1.5$ and $0 \leq \beta \leq 0.7$; see Fig. 6 in Vandermeer 2004), with a resolution of 0.05 for both α and β , and calculated the relative frequency distribution of the phase angles predicted by the model for each point in parameter space. We then minimized the total Euclidean distance between the phase angles predicted by the model and the phase angles derived from the experimental data to find the parameter values that gave the best fit. The best fit of the model to the experimental data was obtained for $\alpha = 1.5$ and $\beta = 0.1$ (compare columns 4 and 5 in Table 1). Interestingly, for these parameter values, the model simulations show considerable variation in the phase angles between the fluctuating species, even though the main phase angles still point at coupling through competition (Table 1). More specifically, the model predicts chaos for this parameter combination of strong coupling through competition (high α) but weak coupling through predation (low β), consistent with the chaotic dynamics observed in the experiment.

DISCUSSION

It is well-known from classic ecological theory that predator–prey interactions can generate oscillations (Lotka 1925; Volterra 1926; Rosenzweig & MacArthur 1963). The existence of predator–prey oscillations predicted by theory has been confirmed by many laboratory experiments and

field observations. Textbook examples of predator–prey oscillations include the famous hare–lynx cycles in northern Canada (Elton & Nicholson 1942; Stenseth *et al.* 1997), Huffaker's (1958) experiments with herbivorous and predatory mite species, and several laboratory experiments with microbial predator and prey species (Gause 1934; Luckinbill 1973; Fussmann *et al.* 2000; Yoshida *et al.* 2003; Becks *et al.* 2005). Food webs typically contain multiple predator and prey species. Thus, food webs provide many opportunities for coupled oscillations driven by the interplay between several predator–prey cycles. Yet, coupled oscillations of multiple predator and prey species have thus far received surprisingly little attention in experimental studies.

Theory predicts that coupled predator–prey oscillations can generate complex dynamics, including chaos (Vandermeer 1993, 2004; Dakos *et al.* 2009). Yet, coupled predator–prey oscillations do not provide the only source of chaos in population dynamics. Models predict that chaos can also be generated by a plethora of other mechanisms, including multispecies competition (Huisman & Weissing 1999, 2001), tritrophic food chains consisting of a prey, predator and top-predator (Hastings & Powell 1991), intraguild predation (Tanabe & Namba 2005), and the interplay between mixing and sinking of plankton populations (Huisman *et al.* 2006). Which of these mechanisms are most relevant for the generation of chaos in natural communities is an important but, as yet, unanswered question. In our experimental system, however, the focus on two coupled predator–prey oscillations arises quite naturally, because the phytoplankton and herbivorous zooplankton were each dominated by two species (picocyanobacteria and nanoflagellates in the phytoplankton, rotifers and calanoid copepods in the herbivorous zooplankton), and their ups and downs resembled typical phytoplankton–zooplankton oscillations (Benincà *et al.* 2008).

Although our study presents the first experimental analysis of two coupled predator–prey oscillations, it has several limitations. First, the population dynamics of the phytoplankton and herbivorous zooplankton species investigated in this paper were embedded in a larger food web, including a top-predator (cyclopoid copepods of the *Eucyclops* genus) and a microbial loop (Benincà *et al.* 2008). We do not know to what extent the coupled oscillations between our focal species may have been influenced by interactions with these other food web components. Second the phytoplankton and zooplankton species in our study will probably have shown considerable intraspecific variation, since the organisms were not obtained from well-defined laboratory clones but were simply scooped up from sea. In addition, calanoid copepods have stage-structured life cycles consisting of naupliar, copepodid and adult stages, and may feed on different prey at different life stages. It is well-known that genetic variation or phenotypic plasticity within

prey species (Abrams & Matsuda 1997; Yoshida *et al.* 2003; Vos *et al.* 2004) and stage-structured variation within predator species (De Roos *et al.* 2003; McCauley *et al.* 2008) can affect the stability of predator–prey interactions, and may modify the phase relationships between predator and prey species.

Despite these limitations, statistical analysis revealed that the time series showed persistent alternations in species dominance. The phytoplankton species composition switched between picocyanobacteria and nanoflagellates, while the zooplankton species composition shifted back and forth between rotifers and calanoid copepods. Moreover, cross-wavelet analysis and wavelet coherence were able to detect significant phase relationships between the ups and downs of the phytoplankton and zooplankton species (Fig. 4, Fig. S4). The time periods with a significant signal covered only a limited part of the time series. However, since the total time series spanned more than 2600 days, the significant signal still covered several hundred days, which is longer than the entire duration of many earlier experimental studies of predator–prey oscillations. During these significant periods, we observed a quarter delay between fluctuations of the predators and their preferred prey species (Table 1). Moreover, the two phytoplankton groups fluctuated in anti-phase (at $\sim 135^\circ$; Table 1), confirming the alternations in species dominance of the phytoplankton. The two zooplankton groups also seemed to fluctuate largely in anti-phase, although for them the pattern was less clear. Comparison between theory and experiment shows that these phase relationships are representative of two coupled predator–prey cycles, with strong coupling through competition but weak coupling through predation (Table 1).

This food web structure is consistent with the size structure of our experimental plankton community. Irrespective of their size, all phytoplankton species compete for the same resources, viz. nutrients and light. Hence, resource competition among phytoplankton species promotes strong coupling through competition. However, small phytoplankton (picocyanobacteria, in our study) are mainly eaten by small zooplankton (rotifers), whereas larger phytoplankton (nanoflagellates) are eaten by larger zooplankton (calanoid copepods). These size differences restrict overlap in the diet of the zooplankton species, which results in weak coupling through predation. Interestingly, comparison of the observed and predicted phase relationships showed that the model parameters yielding the best fit to the experimental data actually predict chaos. This is in agreement with previous analysis, which demonstrated chaos in this food web using a completely independent approach (Benincà *et al.* 2008). The general picture thus emerging from these findings is that the size structure of the plankton in our experimental food web has resulted in two parallel food

chains, one of them consisting of small zooplankton specialized on small phytoplankton and the other of larger zooplankton specialized on larger phytoplankton. The two parallel food chains are weakly coupled through predation, but strongly coupled through phytoplankton competition. Coupling of the predator–prey oscillations in these two parallel food chains has, in turn, contributed to the chaotic nature of the species fluctuations.

Intuitively, it is straightforward to understand why this food web structure, with two predator species specialized on different prey species, leads to continued alternations in species dominance. In essence, coexistence of prey species is achieved through a non-equilibrium version of the ‘killing-the-winner’ mechanism (Thingstad & Lignell 1997; Thingstad 2000). Every time one of the prey species tends to dominance, its key predator shows up, suppresses further population development, and thereby swings the competitive balance to the other prey species. For instance, if picocyanobacteria are abundant, the rotifer population will increase and will suppress the picocyanobacteria. Hence, nanoflagellates can gain a competitive advantage, and will displace the picocyanobacteria. This will benefit the calanoid copepods, which rise in abundance, and subsequently suppress the nanoflagellates. This, in turn, gives new opportunities for picocyanobacteria to seize the available resources. In this way, the system rocks back and forth between the two predator–prey cycles. These non-equilibrium dynamics prevent competitive exclusion, and could therefore play an important role in the maintenance of biodiversity (Huisman & Weissing 1999; Vandermeer 2006; Brose 2008). It would be intriguing to learn whether similar patterns of alternating species dominance can also be observed in other food webs.

ACKNOWLEDGEMENTS

We thank Gilbert Compo, Christopher Torrence and Aslak Grinsted for helpful feedback on the wavelet analysis, Tom van Engeland, Marten Scheffer, Egbert van Nes and Mercedes Pascual for useful discussions, and the anonymous referees for their helpful comments on the manuscript. The investigations of E.B., K.D.J. and J.H. were supported by the Earth and Life Sciences Foundation (ALW), which is subsidized by the Netherlands Organization for Scientific Research (NWO).

REFERENCES

- Abrams, P.A. & Matsuda, H. (1997). Prey adaptation as a cause of predator–prey cycles. *Evolution*, 51, 1742–1750.
- Becks, L., Hilker, F.M., Malchow, H., Jürgens, K. & Arndt, H. (2005). Experimental demonstration of chaos in a microbial food web. *Nature*, 435, 1226–1229.

- Begon, M., Townsend, C.R. & Harper, J.L. (2006). *Ecology: From Individuals to Ecosystems*, 4th edn. Blackwell Publishing, Oxford.
- Benincà, E., Huisman, J., Heerkloss, R., Jöhnk, K.D., Branco, P., Van Nes, E.H. *et al.* (2008). Chaos in a long-term experiment with a plankton community. *Nature*, 451, 822–825.
- Bennett, M., Schatz, M.F., Rockwood, H. & Wiesenfeld, K. (2002). Huygens's clocks. *Proc. Roy. Soc. Lond. A*, 458, 563–579.
- Brose, U. (2008). Complex food webs prevent competitive exclusion among producer species. *Proc. Roy. Soc. Lond. B*, 275, 2507–2514.
- Cazelles, B., Chavez, M., Berteaux, D., Ménard, F., Vik, J.O., Jenouvrier, S. *et al.* (2008). Wavelet analysis of ecological time series. *Oecologia*, 156, 287–304.
- Dakos, V., Benincà, E., van Nes, E.H., Philippart, C.J.M., Scheffer, M. & Huisman, J. (2009). Interannual variability in species composition explained as seasonally entrained chaos. *Proc. Roy. Soc. Lond. B*, 276, 2871–2880.
- De Roos, A.M., Persson, L. & McCauley, E. (2003). The influence of size-dependent life-history traits on the structure and dynamics of populations and communities. *Ecol. Lett.*, 6, 473–487.
- Elton, C. & Nicholson, M. (1942). The ten-year cycle in numbers of the lynx in Canada. *J. Anim. Ecol.*, 11, 215–244.
- Fussmann, G.F., Ellner, S.P., Shertzer, K.W. & Hairston, N.G. Jr (2000). Crossing the Hopf bifurcation in a live predator–prey system. *Science*, 290, 1358–1360.
- Gause, G.F. (1934). *The Struggle for Existence*. Williams & Wilkins, Baltimore.
- Gilman, D.L., Fuglister, F.J. & Mitchell, J.M. Jr (1963). On the power of red noise. *J. Atmos. Sci.*, 20, 182–184.
- Golubitsky, M., Stewart, I., Buono, P.L. & Collins, J.J. (1999). Symmetry in locomotor central pattern generators and animal gaits. *Nature*, 401, 693–695.
- Grenfell, B.T., Bjørnstad, O.N. & Kappey, J. (2001). Travelling waves and spatial hierarchies in measles epidemics. *Nature*, 414, 716–723.
- Grinsted, A., Moore, J.C. & Jevrejeva, S. (2004). Application of cross wavelet transform and wavelet coherence to geophysical time series. *Nonlinear Process Geophys.*, 11, 561–566.
- Hastings, A. & Powell, T. (1991). Chaos in a three-species food chain. *Ecology*, 72, 896–903.
- Heerkloss, R. & Klinkenberg, G. (1998). A long-term series of a planktonic foodweb: a case of chaotic dynamics. *Verh. Int. Ver. Limnol.*, 26, 1952–1956.
- Huffaker, C.B. (1958). Experimental studies on predation: dispersion factors and predator–prey oscillations. *Hilgardia*, 27, 795–835.
- Huisman, J. & Weissing, F.J. (1999). Biodiversity of plankton by species oscillations and chaos. *Nature*, 402, 407–410.
- Huisman, J. & Weissing, F.J. (2001). Biological conditions for oscillations and chaos generated by multispecies competition. *Ecology*, 82, 2682–2695.
- Huisman, J., Pham Thi, N.N., Karl, D.M. & Sommeijer, B. (2006). Reduced mixing generates oscillations and chaos in the oceanic deep chlorophyll maximum. *Nature*, 439, 322–325.
- Keitt, T.H. (2008). Coherent ecological dynamics induced by large scale disturbance. *Nature*, 454, 331–334.
- Keitt, T.H. & Fisher, J. (2006). Detection of scale-specific community dynamics using wavelets. *Ecology*, 87, 2895–2904.
- Kiss, I.Z., Zhai, Y. & Hudson, J.L. (2002). Emerging coherence in a population of chemical oscillators. *Science*, 296, 1676–1678.
- Lotka, A.J. (1925). *Elements of Physical Biology*. Williams & Wilkins, Baltimore.
- Luckinbill, L.S. (1973). Coexistence in laboratory populations of *Paramecium aurelia* and its predator *Didinium nasutum*. *Ecology*, 54, 1320–1327.
- Maraun, D. & Kurths, J. (2004). Cross wavelet analysis: significance testing and pitfalls. *Nonlinear Process Geophys.*, 11, 505–514.
- McCauley, E., Nelson, W.A. & Nisbet, R.M. (2008). Small-amplitude cycles emerge from stage-structured interactions in *Daphnia*–algal systems. *Nature*, 455, 1240–1243.
- Ménard, F., Marsac, F., Bellier, E. & Cazelles, B. (2007). Climatic oscillations and tuna catch rates in the Indian Ocean: a wavelet approach to time series analysis. *Fish. Oceanogr.*, 16, 95–104.
- Rodriguez, E., George, N., Lachaux, J.P., Martinerie, J., Renault, B. & Varela, F.J. (1999). Perception's shadow: long-distance synchronization of human brain activity. *Nature*, 397, 430–433.
- Rosenzweig, M.L. & MacArthur, R.H. (1963). Graphical representation and stability conditions of predator–prey interactions. *Am. Nat.*, 97, 209–223.
- Stenseth, N.C., Falck, W., Bjørnstad, O.N. & Krebs, C.J. (1997). Population regulation in snowshoe hare and Canadian lynx: asymmetric food web configurations between hare and lynx. *Proc. Natl Acad. Sci. USA*, 94, 5147–5152.
- Strogatz, S.H. & Stewart, I. (1993). Coupled oscillators and biological synchronization. *Sci. Am.*, 269, 102–109.
- Tanabe, K. & Namba, T. (2005). Omnivory creates chaos in simple food web models. *Ecology*, 86, 3411–3414.
- Thingstad, T.F. (2000). Elements of a theory for the mechanisms controlling abundance, diversity, and biogeochemical role of lytic bacterial viruses in aquatic systems. *Limnol. Oceanogr.*, 45, 1320–1328.
- Thingstad, T.F. & Lignell, R. (1997). Theoretical models for the control of bacterial growth rate, abundance, diversity and carbon demand. *Aquat. Microb. Ecol.*, 13, 19–27.
- Torrence, C. & Compo, G.P. (1998). A practical guide to wavelet analysis. *Bull. Am. Meteorol. Soc.*, 79, 61–78.
- Vandermeer, J. (1993). Loose coupling of predator–prey cycles: entrainment, chaos, and intermittency in the classic MacArthur consumer–resource equations. *Am. Nat.*, 141, 687–716.
- Vandermeer, J. (2004). Coupled oscillations in food webs: balancing competition and mutualism in simple ecological models. *Am. Nat.*, 163, 857–867.
- Vandermeer, J. (2006). Oscillating populations and biodiversity maintenance. *Bioscience*, 56, 967–975.
- Volterra, V. (1926). Fluctuations in the abundance of a species considered mathematically. *Nature*, 118, 558–560.
- Vos, M., Kooi, B.W., DeAngelis, D.L. & Mooij, W.M. (2004). Inducible defences and the paradox of enrichment. *Oikos*, 105, 471–480.
- Yoshida, T., Jones, L.E., Ellner, S.P., Fussmann, G.F. & Hairston, N.G. Jr (2003). Rapid evolution drives ecological dynamics in a predator–prey system. *Nature*, 424, 303–306.

SUPPORTING INFORMATION

Additional Supporting Information may be found in the online version of this article:

Figure S1 A simple example to illustrate the interpretation of wavelet power spectra.

Figure S2 Examples of a wavelet function.

Figure S3 Wavelet power spectra of the phytoplankton and zooplankton species.

Figure S4 Wavelet coherence of the phytoplankton and zooplankton species.

Table S1 Phase angles between the species fluctuations detected by wavelet coherence analysis.

Appendix S1 Time series of the long-term experiment.

Appendix S2 Wavelet analysis.

As a service to our authors and readers, this journal provides supporting information supplied by the authors. Such materials are peer-reviewed and may be re-organized for online delivery, but are not copy-edited or typeset. Technical support issues arising from supporting information (other than missing files) should be addressed to the authors.

Editor, Andrew Beckerman

Manuscript received 26 June 2009

First decision made 3 August 2009

Manuscript accepted 29 August 2009